Vietnam Journal of Science and Technology ***64***(3) (2026) 528–541
DOI: https://doi.org/10.15625/2525-2518/20566

Combating river pathogens and reducing water pollution in Ulaanbaatar with silver nanoparticles

Altantogos Myagmar[1,2,*], Chuluunbaatar Otgonbaatar[3], Tamara Maamuu[4], Batkhishig Myagmar[5], Sarangerel Davaasambuu[6]

[1]*Department of Chemistry and Biological Engineering, School of Engineering and Applied Sciences, National University of Mongolia, Ulaanbaatar 14201, Mongolia*
[2]*Department of Medical Chemistry, School of Bio-Medicine, Mongolian National University of Medical Sciences, Ulaanbaatar 14210, Mongolia*
[3]*Department of Radiology, College of Medicine, Seoul National University, Seoul 03080, South Korea*
[4]*Division of Theoretical and High Energy Physics, Institute of Physics and Technology, Mongolian Academy of Sciences, Ulaanbaatar 13330, Mongolia*
[5]*Nest Education IT School, Ulaanbaatar 14192, Mongolia*
[6]*Department of Chemistry, School of Arts and Sciences, National University of Mongolia, Ulaanbaatar 14201, Mongolia*

[*]Emails: *altantogos.mg@mnums.edu.mn*

Received: 15 April 2024; Accepted for publication: 6 January 2025

Abstract. Ulaanbaatar, the capital of Mongolia, is dealing with significant water pollution due to rapid urbanization, a dense population, and the widespread use of traditional stoves. With half of Mongolia's population residing in the capital city, the strain on infrastructure results in untreated wastewater entering water bodies, emphasizing the urgent need to reduce pollution for public health and the environment. Our research focuses on utilizing chemical synthesis to prepare silver nanoparticles (Ag NPs) aimed at reducing pathogenic pollutants in river water. We investigated the properties and antibacterial activity of the Ag NPs synthesized through the chemical reduction method of $AgNO_3$ using $NaBH_4$, with polyvinylpyrrolidone (PVP) utilized as a stabilizer to prevent agglomeration. Characterization was performed using a variety of analytical techniques, including UV/Vis spectroscopy, X-ray diffraction (XRD), and NANOPhox particle analysis. The borohydride reduction method yielded Ag NPs with an average particle diameter of 53.69 nm. The silver nanoparticle solution exhibited a yellow color, as observed on a UV/Vis spectrophotometer at a wavelength of 389.5 nm. Furthermore, the Ag NPs demonstrated significant antibacterial activity against *Salmonella typhimurium* (*S. typhimurium*) and drug-resistant *Escherichia coli* (*E. coli*) bacteria.

Keywords: chemical reduction, silver nanoparticles, pathogenic pollutants, polyvinylpyrrolidone, antibacterial activity.

Classification numbers: 3.4, 3.5.

1. INTRODUCTION

Ulaanbaatar, the capital city of Mongolia, faces significant water pollution challenges, primarily stemming from rapid urbanization, a dense population, and the extensive use of traditional stoves in traditional Mongolian house areas. The city's increasing number of people, which comprises half of Mongolia's residents, is putting a strain on the city's infrastructure and sanitation facilities. Consequently, untreated wastewater is being released into water bodies. Effectively reducing water pollution is imperative to safeguard public health and the environment [1–6]. Mitigating water pollution in Ulaanbaatar is crucial not only for improved water quality and enhanced environmental health but also as a significant component of global efforts to address persistent health challenges [4, 5, 7, 8]. The worldwide increase in bacterial infections and the rise of antibiotic resistance have been identified as significant concerns in twenty-first-century biomedicine in recent years [9]. Addressing these challenges requires the research and development of novel antibacterial agents [10]. Nanoparticles (NPs) are considered a promising alternative to antibiotics due to their high potential to address the issues of antibiotic resistance [10–14].

Ag NPs are progressively being employed in various fields, including medical, food, health care, consumer, and industrial purposes, owing to their unique physical and chemical properties. [10, 15, 16]. Nanoparticle synthesis conventionally relies on three distinct approaches: physical, chemical, and biological methods. Chemical methods, utilizing water or organic solvents, have been a common avenue for preparing Ag NPs [17, 18]. This process typically involves three key components: metal precursors, reducing agents, and stabilizing/capping agents [19]. The "top-down" approach entails the mechanical grinding of bulk metals, followed by stabilization using colloidal protecting agents [19, 20]. Chemical methods offer a major advantage in terms of high yield, contrasting with the low yield associated with physical methods. Achieving Ag NPs with a well-defined size is challenging, necessitating additional steps to prevent particle aggregation [21]. Chemical methods encompass a variety of techniques, including cryochemical synthesis, laser ablation, lithography, electrochemical reduction, laser irradiation, sono-decomposition, thermal decomposition, and chemical reduction [22–33]. While chemical synthesis offers advantages such as ease of bulk production, low cost, and high yield [34], various chemical reducers are employed in the synthesis of Ag NPs. These include sodium borohydride ($NaBH_4$) [35–39], hydrazine (N_2H_4) [40–43], citrate (sodium citrate) [44–50], ascorbic acid (vitamin C) [47, 48], polyols (tannic acid, plant extracts rich in bioactive compounds [38], and ammonium hydroxide. Each serves specific roles such as reducing silver ions, stabilizing the synthesis process, or acting as both reducing and capping agents, with green synthesis methods increasingly incorporating biocompatible options like ascorbic acid and plant extracts.

In this study, we utilized the chemical reduction method to synthesize Ag NPs with the aim of reducing pathogenic bacteria in water, particularly targeting infectious gram-negative bacteria including *E. coli* and *S. typhimurium*, which were extracted from river water located in the main settled area in Ulaanbaatar city center, Mongolia.

2. MATERIALS AND METHODS

This section outlines a comprehensive methodology designed for easy replication, detailing the synthesis of silver nanoparticles (Ag NPs) utilizing Sigma-Aldrich chemicals, characterization techniques including UV/Vis spectroscopy and X-ray diffractometry, and antibacterial testing in Selbe River water (47°53'1.3"N, 106°48'51.8"E, Bayanzurkh district,

Ulaanbaatar, Mongolia) using diverse media and colloidal silver solutions, ensuring sterile conditions and clear descriptions of any modifications to established procedures.

2.1. Materials

All chemicals supplied by Sigma-Aldrich were of analytical grade and were used as received without further purification. Silver nitrate (Sigma-Aldrich, 99.0 %) served as the precursor for Ag NPs. Sodium borohydride (Sigma Aldrich, 96.0 %) and, as a stabilizing agent, PVP (Sigma-Aldrich, 99.0 %), were selected, each with an average molecular mass of 40,000 g/mol. Deionized water was used in the experiments, and all glassware was thoroughly cleaned by rinsing with ultrapure water prior to use.

2.2. Methods

The synthesis and characterization of silver nanoparticles involve a systematic process utilizing chemical reduction with sodium borohydride and subsequent analysis through UV/Vis spectroscopy, X-ray diffractometry, and particle size determination techniques.

2.2.2. Synthesis of silver nanoparticles

The process of synthesizing nano-sized silver through chemical reduction with thestrong reducing agent sodium borohydride began with the preparation of aqueous solutions of 0.001 M silver nitrate ($AgNO_3$) and 0.002 M sodium borohydride ($NaBH_4$). The experiment was continued by taking 30 mL of 0.002 M sodium borohydride solution and cooling it to 10 °C in an ice bath. The cooled solution was stirred at 80 rpm on an MSH-20D magnetic stirrer (Korea), then 10 mL of 0.001 M silver nitrate solution were added dropwise using a burette. The resulting solution was then dried using a lyophilizer (FD-12 Lab Freeze Dryer/lyophilizer, China), yielding the prepared dry sample. The synthesized Ag NPs were stabilized by adding 20 mL of a 0.3 % PVP solution and stored in a refrigerator at 4 °C for preservation.

2.2.3. Characterization of silver nanoparticles

During the characterization process, a range of analytical techniques were employed, encompassing UV/Vis spectroscopy, XRD, and NANOPhox particle size analysis. The average particle diameter, viscosity and refractive index of the synthesized nanoparticles were determined using a Nanophox NX0061 instrument (Simpatec, Germany). The UV/Visible spectra of Ag NPs were recorded using a UV-2550 spectrometer (Shimadzu, Japan) with a 1 cm path length quartz cell in the range of 200–800 nm. Measurements were conducted immediately after preparing the Ag NPs and 21 days after synthesis. XRD patterns were obtained using a MAXima XRD-7000 diffractometer (Shimadzu, Japan) in the 2θ range from 30 to 80°, employing a scan speed of 0.02°/sec, powered by an α-Cu X-ray tube operating at 40 kV and 30 mA.

2.2.4. Antibacterial test

The methodology encompassed river water sampling from the Selbe River according to standardized protocols, subsequent media preparation, and antibacterial testing involving bacterial culture in both control and silver colloid solution-amended media, followed by identification and assessment of bacterial growth rates, ensuring sterility and precise experimental conditions.

2.2.4.1. Collecting river water samples

For the research work, samples were taken from the Selbe River in Ulaanbaatar city following the Mongolian standard MNS 5667-6:2001, which is equivalent to ISO 5667-5:2006, titled "Water quality - Sampling Part 6: Guidance on Sampling of Rivers and Streams". We subsequently determined main ions constituents of the water. The results of the Selbe River water analysis include: NH_4^+ at 1.3 mg/L, Ca^{2+} at 120.24 mg/L, and Mg^{2+} at 23.085 mg/L, contributing to a total cation concentration of 144.625 mg/L. The anion concentrations include: Cl^- at 76.9265 mg/L, SO_4^{2-} at 93.82 mg/L, NO_2^- at 0.6 mg/L, NO_3^- at 72.58 mg/L, and HCO_3^- at 292.8768 mg/L, resulting in a total anion concentration of 536.8033 mg/L. The Selbe River water analysis indicates that the water is classified as "moderately hard" according to the World Health Organization's standards, with calcium carbonate concentrations ranging from 60 to 120 mg/L [68, 69].

2.2.4.2. Media preparation

Meat peptone broth (MPB): For the preparation of MPB, 13 g of nutrient broth, 3 g of yeast extract powder, and 5 g of peptone were combined in 1 L of distilled water. The pH of the mixture was adjusted to 7.4 +/- 0.2. The medium was sterilized at 121 °C for 15 minutes. Finally, a sterile solution of $CaCl_2$ (stock solution, 0.02 M) was added to achieve a final concentration of 0.002 M.

Urinary tract infection (UTI, Product description: 30374, Sigma Aldrich): The agar medium was prepared by adding 55.4 g of agar to 1 L of distilled water and boiling to dissolve it completely. Next, the medium was sterilized by autoclaving at a pressure of 1 bar (121 °C) for 15 minutes. The sterile mixture was then cooled to 50 °C and poured into sterile Petri plates.

MacConkey agar (Product number: M8552, Sigma Aldrich): This was prepared by weighing 40 g of agar, consisting of 20.00 g of peptic digest of animal tissue, 10.00 g of lactose, 5.00 g of bile salts, 5.00 g of sodium chloride, and 0.075 g of neutral red. Thorough mixing was performed, and the mixture was subsequently dissolved in distilled water to ensure complete dissolution. The medium underwent sterilization through autoclaving under appropriate conditions. The final pH of the medium was carefully adjusted to 7.4 ± 0.2.

Yeast extract agar (Product description: 01497, Sigma Aldrich): Suspended in 1 L of purified water were 23 g of the medium, which was heated with frequent agitation and boiled for one minute to ensure complete dissolution. The mixture was then autoclaved at 121 °C for 15 minutes and subsequently cooled to 45-50 °C.

Brilliant green agar (Code: CM0263, Thermo fisher scientific): 58.09 g were suspended in 1 L of purified/distilled water. The mixture was heated to boiling to ensure complete dissolution of the medium. Sterilization was performed by autoclaving at 121 °C for 15 minutes. Once sterilized, the solution was cooled to 45-50 °C, thoroughly mixed, then poured into sterile Petri plates.

2.2.4.3. Antibacterial test

The antibacterial test initiation involved assessing bacteria in Selbe River water using both MPB and UTI media. Subsequently, for bacterial detection in a 1 mL water sample, the total bacterial count was determined by incubating at 37 °C for 24 h. The cultured bacteria were then selected and underwent additional culturing on various nutrient media, including MPB, MacConkey, and yeast extract agar, enabling the separate identification of bacteria present in the water.

In a parallel procedure, the pre-prepared and frozen MPB, MacConkey, and yeast extract agar media were thawed in a Petri dish and cooled to 45 °C. Subsequently, 1 mL of the water sample was added to the thawed media for bacterial culture. Simultaneously, a mixture of 1 mL of the water sample and 0.0003 mL of the silver colloid solution was prepared and added to the thawed media. A comparative analysis was then conducted between the media with and without the addition of the silver colloid solution.

Following this, we identified extracted Gram-negative bacterial strains, focusing on two common pathogenic bacteria in water, *E. coli* and *S. typhimurium,* and *S. aureus, E. faecalis,* and *coliform* bacteria, previously isolated from Selbe River water and cultured in McConkey medium. Bacterial cultures were exposed to colloidal silver solutions (0.3, 0.5, 1, 3, 5 mL) at precise concentrations of 5000, 50,000, 500,000, 5,000,000, 50,000,000 cells, respectively, and then incubated at 37 °C for 24 h. All materials used in experiments involving bacteria were sterilized, and zeolite was applied immediately after preparation. Variable amounts of Ag zeolite were then added to the culture, and the colonies were measured over a time course. Bacterial growth rates were determined by counting the number of surviving colonies on selected agar.

3. RESULTS AND DISCUSSION

This section explores the synthesis and characterization of silver nanoparticles, emphasizing the importance of employing protective agents such as PVP for stabilization and discussing the impact of concentration regulation on antibacterial efficacy.

3.1. Characteristics of Ag NPs and their stability

The Ag NPs were successfully synthesized using the chemical reduction method for nanoparticle synthesis, utilizing the strong reducing agent $NaBH_4$ in aqueous solutions. The formation of Ag NPs was confirmed by a change in color from completely colorless to light orange (yellowish), as shown in Figure 1a. In aqueous solution, the reduction of silver ions (Ag^+) typically results in colloidal silver with a particle diameter of several nanometers [18]. When different complexes are initially reduced with Ag^+ ions, silver atoms (Ag) are formed, which then aggregate into oligomeric clusters [39, 40]. These clusters ultimately give rise to the formation of colloidal Ag NPs [41,42].

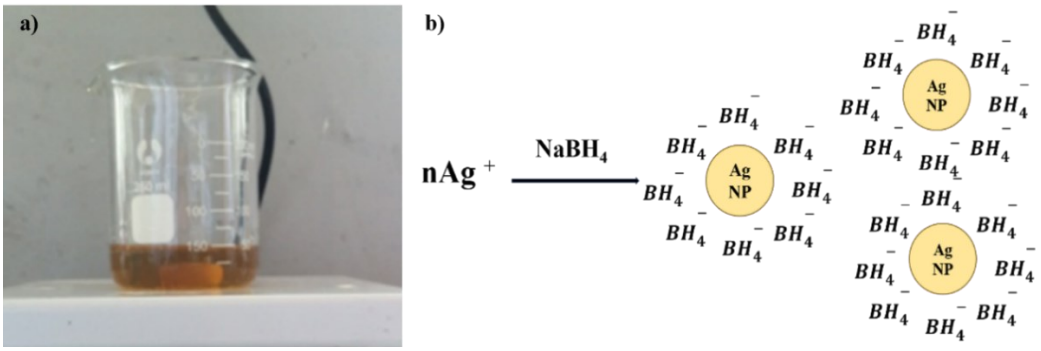

Figure 1. a) Synthesized Ag NPs and b) Structure of Ag NPs in aqueous solution.

In the presence of borohydride anions, silver ions in solution are encircled, creating an ionic circle with a negatively charged surface as shown in Figure 1b [66]. The possibility to store chemically synthesized NPs for later use is crucial for various applications [65].

The average particle diameter of the synthesized Ag NPs was determined using a NANOPhox instrument and is shown as 53.69 nm in Figure 2. Additionally, the refractive index of the colloidal solution containing silver nanoparticles was 1.333, and the viscosity measured was 0.890 mPa. The silver nanoparticle solution, featuring a refractive index of 1.333, is similar to that of water at 20 °C. The silver nanoparticle solution exhibits a viscosity of 0.89 mPa, contrasting with water's viscosity of 1.002 mPa·s at the same temperature. This difference indicates a lower viscosity for the silver nanoparticle solution, implying reduced resistance to flow.

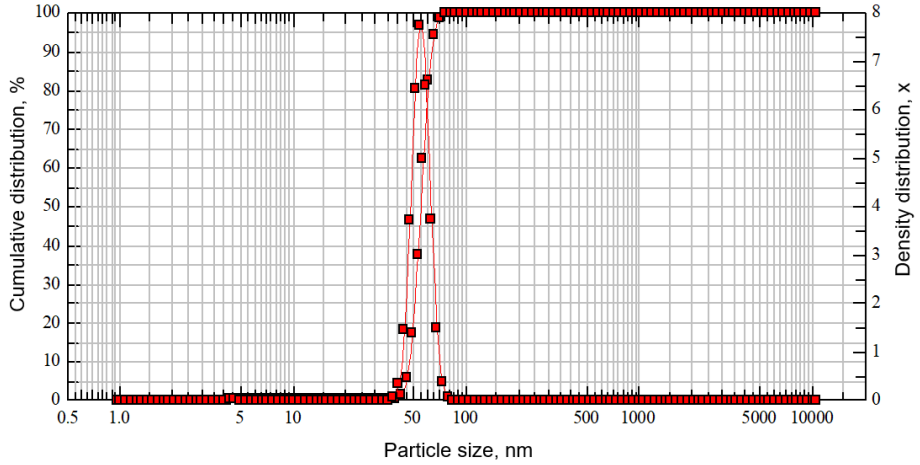

Figure 2. Average distribution and average diameter of synthesized Ag NPs.

In investigating the stability of Ag NPs, the color of the reaction mixture was monitored and the absorption spectra were measured. The initial orange appearance of the silver colloid solution was attributed to the influence of the stabilizing PVP reagent as shown in Figure 3a. The color progressively changed to red during the period of 7 and 21 days, as seen in Figures 3b to 3d.

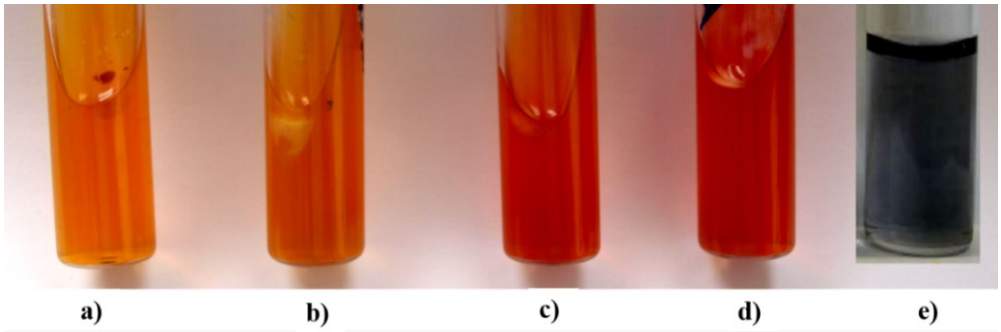

Figure 3. Synthesized silver colloid solution is presented at different stages: a) immediately after synthesis with PVP, b) Ag NPs with PVP after 7, 14 (c), and 21 days (d), and e) Ag NPs without PVP after 21 days.

However, if not adding PVP reagent after 21 days, silver was oxidized, black precipitate of silver oxide was formed, and the filtrate became clear as shown in Figure 3e. The Ag NPs were not agglomerated, proving that PVP has a stabilizing effect on the solution. This phenomenon is further clarified by the arrangement of the second bond of the C=O group of PVP and the pair of electrons on the outer layer of nitrogen being on the same plane, inducing a mesomeric effect that results in an increased negative charge on the oxygen atom and a positive charge on the nitrogen atom (Figure 4a) [43-45].

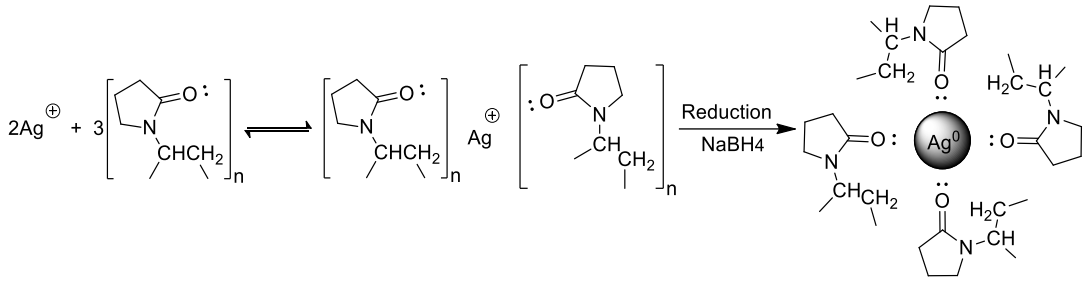

Figure4. Effect of PVP in solution and its interaction mechanism with silver colloid during nanoparticle formation.

The repetitive units within PVP play a pivotal role in stabilizing these nanoparticles, preventing undesired agglomeration and uncontrolled growth as shown in Figure 4. The absorption spectrum of the freshly synthesized silver colloid solution reveals a peak light absorption at a wavelength of 389.5 nm, similar to the results of Mirzaei, as illustrated in Figure 5a [42-44].

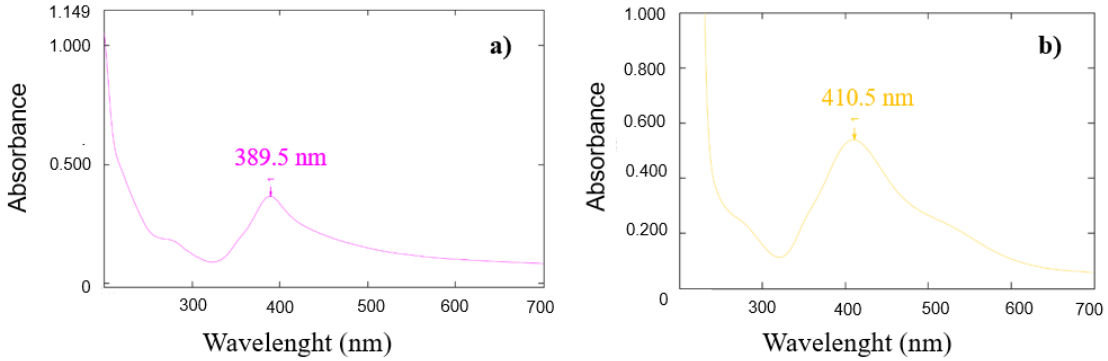

Figure 5. UV/Vis spectra of Ag NPs: a) Synthesized particles, and b) PVP-stabilized particles.

However, the maximum light absorption gradually shifts to 410.5 nm due to the influence of the stabilizer and PVP, as shown in Figure 5b. The observed shift in the maximum light absorption from 389.5 nm to 410.5 nm in the absorption spectrum of the freshly synthesized silver colloid solution is attributed to factors such as stabilizer influence and chemical interactions. As shown in Figure 4, which likely elucidates the charge transfer process, it becomes evident that the multiple repeating polymer units of PVP significantly influence the interaction between the polymer and the silver nanoparticle surface. This simplicity contributes to the production of clean and well-defined silver nanoparticle composites. In summary, PVP acts as a stabilizing agent during the synthesis of Ag/PVP composites, preventing agglomeration of silver nanoparticles and influencing charge transfer processes [43, 45-47]. The synthesis

method described offers advantages in terms of simplicity and the elimination of additional additives, enhancing the appeal of this approach for the fabrication of precisely engineered silver nanoparticle composites.

3.2. XRD analysis of Ag NPs

The XRD analysis of silver nanoparticles revealed characteristic diffraction peaks corresponding to the crystalline structure of metallic silver. The phase analysis of the nanoparticles was determined through XRD, as illustrated in Figure 6. The XRD analysis of silver nanoparticles exhibited distinct diffraction peaks at 2θ values of 38.2, 39.46, 44.3, 64.5, and 77.8°, corresponding to the (111), (200), (220), and (311) crystallographic planes of metallic silver (JCDPS File No. 04-0783). All peaks observed in the XRD pattern can be confidently indexed as a face-centered cubic structure.

The sharp XRD peaks indicate the high crystalline structure of the as-prepared Ag NPs, and the absence of other peaks attributed to $AgNO_3$ or other compounds suggests high purity of the Ag product.

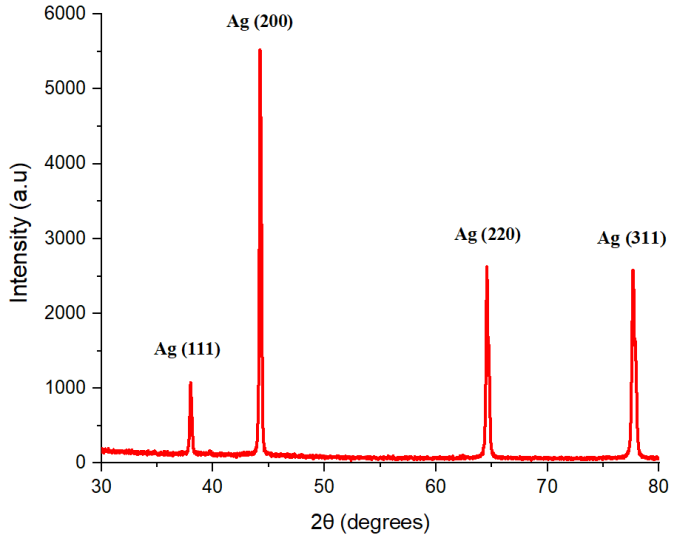

Figure 6. XRD pattern of Ag NPs.

3.3. Antibacterial activity of Ag NPs

The antimicrobial efficacy of Ag NPs is essential for infection prevention in medical fields, optimizing public health via hygiene applications, ensuring water sanitation, fortifying food safety, and aiding in the mitigation of antibiotic resistance. The effective antibacterial properties of silver nanoparticles allow for efficient bacterial disinfectant and improve the general quality of water when used in water sanitation. In our study, we assessed the presence of waterborne bacteria through thorough analyses, further confirming the ability of silver nanoparticles to reduce microbial contaminants and enhance water safety. In Figure 7, the common bacteria in the Selbe River are illustrated on MPB medium.

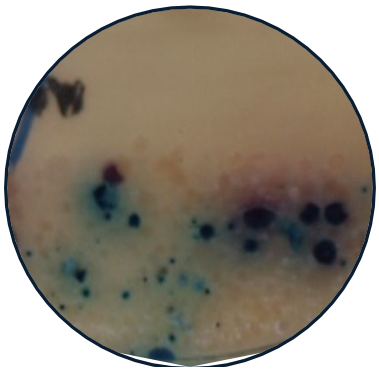

Figure 7. Total bacteria in water samples cultured in MPB media.

During the cultivation of total bacteria from the water in the nutrient medium, various bacterial types were observed. *E. coli*, *S. aureus*, *Enterococcus faecalis (E. faecalis)*, and *Salmonella typhimurium (S. typhimurium)* have been detected in the water of the Selbe River, prompting concerns about potential health risks associated with fecal contamination and waterborne pathogens. Blue-purple slimy bacteria, exhibiting a rough texture and existing either in separated or paired forms resembling *E. coli,* coexisted with small clear white bacteria, bipolar single and double coliform bacteria. *S. aureus*, identified as greenish-blue *cocci* and *bacilli*, was also detected, while *E. faecalis*, a large white-gray bacterium, was tentatively considered to be *S. typhimurium* (refer to Figure 7). After re-inoculating water samples into McConkey medium, two distinct bacterial phenotypes became apparent. McConkey characterized the red and opaque colonies as representative of *E. coli,* while the subsequent growth, marked by gray and rough colonies, was identified as *S. typhimurium*. The results presented in Figure 8 illustrate key findings or observations relevant to the study. Waterborne infectious diseases are closely related to environmental factors, particularly involving water and infection. Epidemiological studies of epidemic and endemic outbreaks of gastrointestinal illness associated with untreated water primarily point to bacteria and viruses, including *E. coli*, *S. typhimurium*, *Shigella*, and norovirus [48, 49].

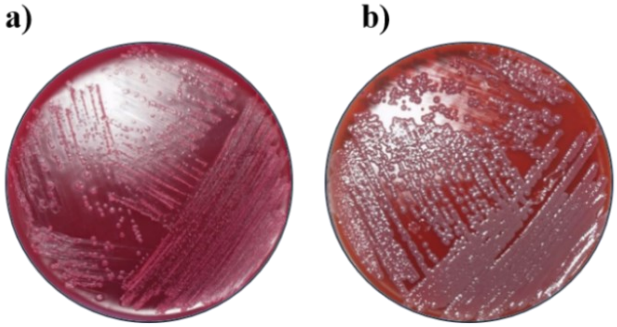

Figure 8. Bacterial growth on McConkey medium, with (a) highlighting *E. coli* bacteria and (b) portraying *S. typhimurium* bacteria.

In the medium of yeast extract agar, a small, transparent, pale-gray, slimy bacterium was identified as *S. aureus*, as illustrated in Figure 9a. On the brilliant green medium, a small, moist colony with a yellow to pale yellow base grew, which was identified as *S. typhimurium* (Figure 9c). This reconfirmed the growth of *S. typhimurium* bacteria grown on McConkey's medium (Figure 9b).

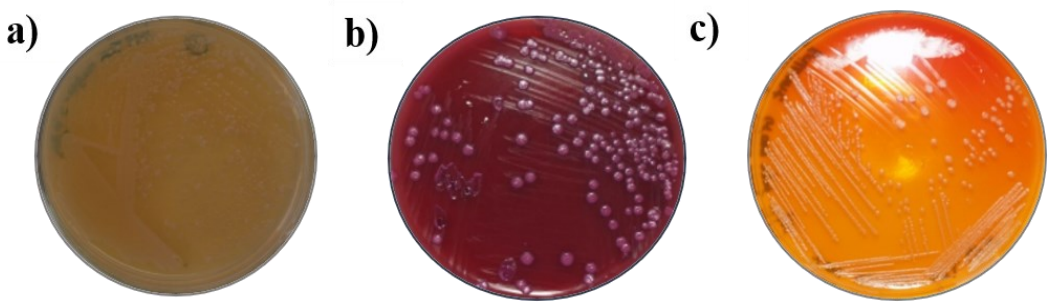

Figure 9. a) *S. aureus* grown on yeast extract agar, b) *S. typhimurium* bacteria grown in McConkey's medium, c) *S. typhimurium* bacteria grown in brilliant green medium.

On brilliant green medium, small moist colonies were isolated with yellow to pale yellow bases, and the bacteria that grew were pale bacteria with pinkish purple bases. It was identified as *S. typhimurium* (Figure 9c). After identifying waterborne bacteria, we specifically chose *E. coli* and *S. typhimurium* for analyzing the health effects of Ag NPs.

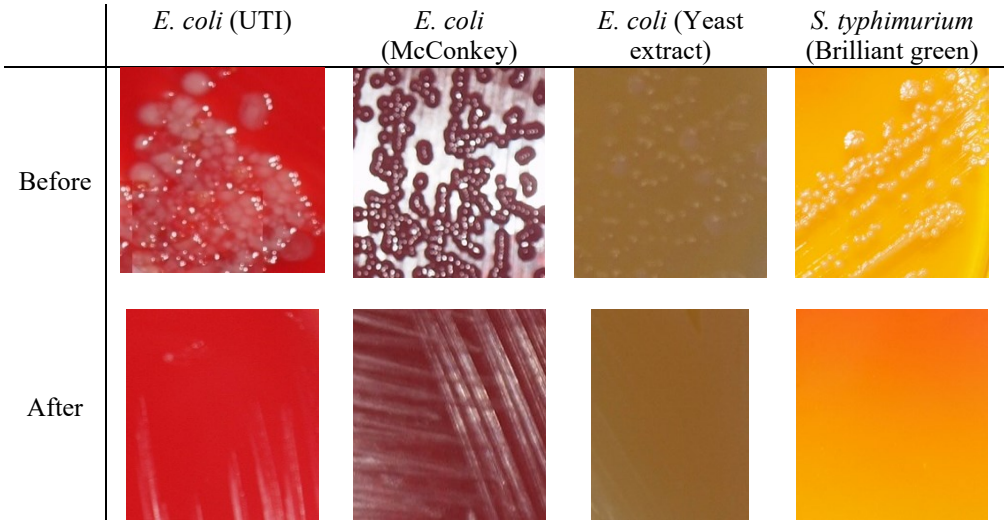

Figure 10. Antibacterial activity of colloidal silver solution against Selbe river water, compared with untreated cultures.

E. coli bacteria were cultured in UTI medium, McConkey medium, and yeast extract medium, while *S. typhimurium* was cultured in brilliant green medium. The cultures were incubated for 24 hours at 35 °C. Before the addition of the silver colloid solution to the water, bacterial growth was observed for both *E. coli* and *S. typhimurium* across all media. After the introduction of the silver colloid solution, no bacterial growth was detected, demonstrating the solution's effectiveness in eliminating bacteria from the water (Figure 10). The experiment primarily focused on bacterial cultures in McConkey medium.

Table 1. Relationship between bacterial dose and silver colloid solution concentration.

Volume of the Ag NPs, mL	Type of bacteria	Bacterial thickening						
		$5{\cdot}10^{9}$	$5{\cdot}10^{8}$	$5{\cdot}10^{7}$	$5{\cdot}10^{6}$	$5{\cdot}10^{5}$	$5{\cdot}10^{4}$	$5{\cdot}10^{3}$

0.3	*E. coli*	+	+	24 h	8 h	4 h	-	-
	S. typhimurium	+	+	24 h	8 h	4 h	-	-
0.5	*E. coli*	+	4 h	-	-	-	-	-
	S. typhimurium	+	+	8 h	-	-	-	-
1.0	*E. coli*	4 h	-	-	-	-	-	-
	S. typhimurium	+	+	8 h	-	-	-	-
2.0	*E. coli*	4 h	-	-	-	-	-	-
	S. typhimurium	+	8 h	-	-	-	-	-
3.0	*E. coli*	4 h	-	-	-	-	-	-
	S. typhimurium	4 h	-	-	-	-	-	-
5.0	*E. coli*	4 h	-	-	-	-	-	-
	S. typhimurium	4 h	-	-	-	-	-	-

+ Resistant strains of E. coli and S. Typhimurium persisted in specific instances within standard samples.
- Complete eradication was observed for both E. coli and S. typhimurium bacteria in standard bacterial samples.

The experimental investigation into the antibacterial activity of varying volumes of Ag NPs against *E. coli* and *S. typhimurium* bacteria revealed distinctive responses. At a concentration of 0.3 mL, both bacterial strains exhibited positive responses, with bacterial thickening observed over 24 h for *E. coli* and 8 h for *S. typhimurium*. However, as the concentration increased, different patterns emerged. For *E. coli*, higher concentrations (1.0 mL, 2.0 mL, 3.0 mL, 5.0 mL) led to bacterial thickening within 4 h, while *S. typhimurium* displayed a similar trend only at 5.0 mL. Interestingly, at 0.5 mL, *E. coli* showed positive responses within 4 h, while *S. typhimurium* exhibited bacterial thickening after 8 h. Moreover, concentrations of 1.0 mL and 2.0 mL resulted in bacterial thickening only for *S. typhimurium*, indicating differential sensitivities between the two bacterial strains. Both strains' lack of bacterial thickening at higher doses implies a potential inhibitory effect on bacterial development. The various response times and concentration-dependent changes highlight the complexities of the interaction between Ag NPs and bacteria. This research highlights the importance of properly regulating Ag NP concentrations to modify antibacterial properties and shows how significant it is to understand the specific details when implementing antimicrobial applications.

4. CONCLUSIONS

Silver nanoparticles play a crucial role in combating common pathogenic bacteria in water, and our accomplishment in producing them using the reduction method is a significant step forward in addressing harmful pathogens in river water. Ag NPs were successfully synthesized using the chemical reduction method with $NaBH_4$, allowing precise control over particle size and resulting in Ag NPs with an average diameter of 53.69 nm. The stabilizing agent, polyvinylpyrrolidone, kept the colloidal solution stable, preventing agglomeration. X-ray diffraction analysis affirmed the face-centered cubic structure of the Ag NPs, indicating high crystallinity and purity. The antibacterial activity of Ag NPs against *E. coli* and *S. typhimurium* exhibited concentration-dependent responses, highlighting the intricate interaction between nanoparticles and bacteria. In conclusion, this research provides valuable insights into the synthesis, stability, and antibacterial properties of Ag NPs, opening avenues for potential applications in medicine, water sanitation, and food safety.

CRediT authorship contribution statement. Altantogos Myagmar: Conceptualization, Investigation, Formal analysis, Writing – original draft, Writing – review & editing, Supervision. Chuluunbaatar Otgonbaatar: Investigation, Formal analysis, Methodology, Writing – original draft. Tamara Maamuu:

Investigation, Formal analysis, Writing – original draft, Writing – review & editing. Batkhishig Myagmar: Investigation, Writing – original draft, Writing – review & editing, Supervision. Sarangerel Davaasambuu: Conceptualization, Methodology, Writing – original draft, Writing – review & editing, Supervision.

Declaration of competing interest. The authors declare that they have no competing interests.

REFERENCES

1. Park H., Fan P., John R., Ouyang Z., Chen J. – Spatiotemporal changes of informal settlements: Ger districts in Ulaanbaatar, Mongolia. Landsc. Urban Plan., **191** (2019) 103630. https://doi.org/10.1016/j.landurbplan.2019.103630.
2. Rahman M. N. – Urban expansion analysis and land use changes in Rangpur city corporation area, Bangladesh, using remote sensing (RS) and geographic information system (GIS) techniques. Geosf. Indones., **4** (2019) 217. https://doi.org/10.19184/geosi.v4i3.13921.
3. Bartram J., Cairncross S. – Hygiene, sanitation, and water: forgotten foundations of health. PLoS Med., **7** (2010) e1000367. https://doi.org/10.1371/journal.pmed.1000367.
4. Lin L., Yang H., Xu X. – Effects of water pollution on human health and disease heterogeneity: a review. Front. Environ. Sci., **10** (2022). https://doi.org/10.3389/fenvs.2022.880246.
5. Soyol-Erdene T.-O., Ganbat G., Baldorj B. – Urban air quality studies in Mongolia: pollution characteristics and future research needs. Aerosol Air Qual. Res., **21** (2021) 210163. https://doi.org/10.4209/aaqr.210163.
6. Annunziato G. – Strategies to overcome antimicrobial resistance (AMR) making use of non-essential target inhibitors: a review. Int. J. Mol. Sci., **20** (2019) 5844. https://doi.org/10.3390/ijms20235844.
7. Salam Md. A., Al-Amin Md. Y., Salam M. T., Pawar J. S., Akhter N., Rabaan A. A., Alqumber M. A. A. – Antimicrobial resistance: a growing serious threat for global public health. Healthcare, **11** (2023) 1946. https://doi.org/10.3390/healthcare11131946.
8. Chinemerem Nwobodo D., Ugwu M. C., Oliseloke Anie C., Al-Ouqaili M. T. S., Chinedu Ikem J., Victor Chigozie U., Saki M. – Antibiotic resistance: the challenges and some emerging strategies for tackling a global menace. J. Clin. Lab. Anal., **36** (2022). https://doi.org/10.1002/jcla.24655.
9. Uddin T. M., Chakraborty A. J., Khusro A., Zidan B. R. M., Mitra S., Emran T. B., Dhama K., Ripon Md. K. H., Gajdács M., Sahibzada M. U. K., et al. – Antibiotic resistance in microbes: history, mechanisms, therapeutic strategies and future prospects. J. Infect. Public Health, **14** (2021) 1750–1766. https://doi.org/10.1016/j.jiph.2021.10.020.
10. Anderson M., Panteli D., van Kessel R., Ljungqvist G., Colombo F., Mossialos E. – Challenges and opportunities for incentivising antibiotic research and development in Europe. Lancet Reg. Health Eur., **33** (2023) 100705. https://doi.org/10.1016/j.lanepe.2023.100705.
11. Adeniji O. O., Nontongana N., Okoh J. C., Okoh A. I. – The potential of antibiotics and nanomaterial combinations as therapeutic strategies in the management of multidrug-resistant infections: a review. Int. J. Mol. Sci., **23** (2022) 15038. https://doi.org/10.3390/ijms232315038.
12. Rudramurthy G., Swamy M., Sinniah U., Ghasemzadeh A. – Nanoparticles: alternatives against drug-resistant pathogenic microbes. Molecules, **21** (2016) 836. https://doi.org/10.3390/molecules21070836.
13. Wang L., Hu C., Shao L. – The antimicrobial activity of nanoparticles: present situation and prospects for the future. Int. J. Nanomedicine, **Volume 12** (2017) 1227–1249. https://doi.org/10.2147/ijn.s121956.
14. Zhang X.-F., Liu Z.-G., Shen W., Gurunathan S. – Silver nanoparticles: synthesis, characterization, properties, applications, and therapeutic approaches. Int. J. Mol. Sci., **17** (2016) 1534. https://doi.org/10.3390/ijms17091534.
15. Wiley B., Sun Y., Mayers B., Xia Y. – Shape-controlled synthesis of metal nanostructures: the case of silver. ChemInform, **37** (2005). https://doi.org/10.1002/chin.200604220.

16. Tao A., Sinsermsuksakul P., Yang P. – Polyhedral silver nanocrystals with distinct scattering signatures. Angew. Chem. Int. Ed., **45** (2006) 4597–4601. https://doi.org/10.1002/anie.200601277.
17. Deepak V., Umamaheshwaran P. S., Guhan K., Nanthini R. A., Krithiga B., Jaithoon N. M. H., Gurunathan S. – Synthesis of gold and silver nanoparticles using purified URAK. Colloids Surf. B Biointerfaces, **86** (2011) 353–358. https://doi.org/10.1016/j.colsurfb.2011.04.019.
18. Mallick K., Witcomb M. J., Scurrell M. S. – Polymer stabilized silver nanoparticles: a photochemical synthesis route. J. Mater. Sci., **39** (2004) 4459–4463. https://doi.org/10.1023/b:jmsc.0000034138.80116.50.
19. Malik M. A., O'Brien P., Revaprasadu N. – A simple route to the synthesis of core/shell nanoparticles of chalcogenides. Chem. Mater., **14** (2002) 2004–2010. https://doi.org/10.1021/cm011154w.
20. Sergeev B. M., Kasaikin V. A., Litmanovich E. A., Sergeev G. B., Prusov A. N. – Cryochemical synthesis and properties of silver nanoparticle dispersions stabilised by poly(2-dimethylaminoethyl methacrylate). Mendeleev Commun., **9** (1999) 130–131. https://doi.org/10.1070/mc1999v009n04abeh001080.
21. Mafuné F., Kohno J., Y., Takeda Y., Kondow T., Sawabe H. – Formation and size control of silver nanoparticles by laser ablation in aqueous solution. J. Phys. Chem. B, **104** (2000) 8334–8337. https://doi.org/10.1021/jp001336y.
22. Hulteen J. C., Treichel D. A., Smith M. T., Duval M. L., Jensen T. R., Van Duyne R. P. – Nanosphere lithography: size-tunable silver nanoparticle and surface cluster arrays. J. Phys. Chem. B, **103** (1999) 3854–3863. https://doi.org/10.1021/jp9904771.
23. Zhu J.-J., Liao X.-H., Zhao X.-N., Chen H.-Y. – Preparation of silver nanorods by electrochemical methods. Mater. Lett., **49** (2001) 91–95. https://doi.org/10.1016/s0167-577x(00)00349-9.
24. Abid J. P., Wark A. W., Brevet P. F., Girault H. H. – Preparation of silver nanoparticles in solution from a silver salt by laser irradiation. Chem. Commun., **7** (2002) 792–793. https://doi.org/10.1039/b200272h.
25. Talebi J., Halladj R., Askari S. – Sonochemical synthesis of silver nanoparticles in Y-zeolite substrate. J. Mater. Sci., **45** (2010) 3318–3324. https://doi.org/10.1007/s10853-010-4349-z.
26. Hosseinpour-Mashkani S. M., Ramezani M. – Silver and silver oxide nanoparticles: synthesis and characterization by thermal decomposition. Mater. Lett., **130** (2014) 259–262. https://doi.org/10.1016/j.matlet.2014.05.133.
27. Q. Z., N. L., J. G., Z. L., Y Y. – A systematic study of the synthesis of silver nanoplates: is citrate a 'magic' reagent? J. Am. Chem. Soc., **133** (2011) 16132–16141. https://doi.org/10.1021/ja2080345.
28. Ganaie S. U., Abbasi T., Abbasi S. A. – Green synthesis of silver nanoparticles using an otherwise worthless weed mimosa (*Mimosa pudica*): feasibility and process development toward shape/size control. Part. Sci. Technol., **33** (2015) 638–644. https://doi.org/10.1080/02726351.2015.1016644.
29. Gurunathan S., Han J., Park J. H., Kim J.-H. – A green chemistry approach for synthesizing biocompatible gold nanoparticles. Nanoscale Res. Lett., **9** (2014) 248. https://doi.org/10.1186/1556-276x-9-248.
30. Gurunathan S., Woong Han J., Kim J. – Green chemistry approach for the synthesis of biocompatible graphene. Int. J. Nanomedicine, **8** (2013) 2719. https://doi.org/10.2147/ijn.s45174.
31. Lingaraju K., Raja Naika H., Nagaraju G., Nagabhushana H. – Biocompatible synthesis of reduced graphene oxide from *Euphorbia heterophylla* (l.) and their *in-vitro* cytotoxicity against human cancer cell lines. Biotechnol. Rep., **24** (2019) e00376. https://doi.org/10.1016/j.btre.2019.e00376.
32. Gurunathan S., Han J. W., Kim E., Park J. H., Kim J.-H. – Reduction of graphene oxide by resveratrol: a novel and simple biological method for the synthesis of an effective anticancer nanotherapeutic molecule. Int. J. Nanomedicine, **10** (2015) 2951. https://doi.org/10.2147/ijn.s79879.
33. Shikha S., Dureja S., Sapra R., Babu J., Haridas V., Pattanayek S. K. – Interaction of borohydride stabilized silver nanoparticles with sulfur-containing organophosphates. RSC Adv., **11** (2021) 32286–32294. https://doi.org/10.1039/d1ra06911j.
34. Eka Putri G., Rahayu Gusti F., Novita Sary A., Zainul R. – Synthesis of silver nanoparticles used chemical reduction method by glucose as reducing agent. J. Phys. Conf. Ser., **1317** (2019) 012027. https://doi.org/10.1088/1742-6596/1317/1/012027.

35. Leiner M. J. P., Hartmann P. – Theory and practice in optical pH sensing. Sens. Actuators B Chem., **11** (1993) 281–289. https://doi.org/10.1016/0925-4005(93)85266-d.
36. Sastry M., Mayya K. S., Bandyopadhyay K. – pH Dependent changes in the optical properties of carboxylic acid derivatized silver colloidal particles. Colloids Surf. A Physicochem. Eng. Asp., **127** (1997) 221–228. https://doi.org/10.1016/s0927-7757(97)00087-3.
37. Naganthran A., Verasoundarapandian G., Khalid F. E., Masarudin M. J., Zulkharnain A., Nawawi N. M., Karim M., Che Abdullah C. A., Ahmad S. A. – Synthesis, characterization and biomedical application of silver nanoparticles. Materials, **15** (2022) 427. https://doi.org/10.3390/ma15020427.
38. Abou El-Nour K. M. M., Eftaiha A., Al-Warthan A., Ammar R. A. A. – Synthesis and applications of silver nanoparticles. Arab. J. Chem., **3** (2010) 135–140. https://doi.org/10.1016/j.arabjc.2010.04.008.
39. Wang H., Qiao X., Chen J., Wang X., Ding S. – Mechanisms of PVP in the preparation of silver nanoparticles. Mater. Chem. Phys., **94** (2005) 449–453. https://doi.org/10.1016/j.matchemphys.2005.05.005.
40. Rónavári A., Bélteky P., Boka E., Zakupszky D., Igaz N., Szerencsés B., Pfeiffer I., Kónya Z., Kiricsi M. – Polyvinyl-pyrrolidone-coated silver nanoparticles-the colloidal, chemical and biological consequences of steric stabilization under biorelevant conditions. Int. J. Mol. Sci., **22** (2021) 8673. https://doi.org/10.3390/ijms22168673.
41. Gharibshahi L., Saion E., Gharibshahi E., Shaari A. H., Matori K. A. – Influence of poly(vinylpyrrolidone) concentration on properties of silver nanoparticles manufactured by modified thermal treatment method. PLoS One, **12** (2017) e0186094. https://doi.org/10.1371/journal.pone.0186094.
42. Mirzaei A., Janghorban K., Hashemi B., Bonyani M., Leonardi S. G., Neri G. – Characterization and optical studies of PVP-capped silver nanoparticles. J. Nanostruct. Chem., **7** (2017) 37–46. https://doi.org/10.1007/s40097-016-0212-3.
43. Perumal R., Casale S., de Stefano L., Spadavecchia J. – Synthesis and characterization of Ag-Protoporphyrin nano structures using mixed co-polymer method. Front. Lab. Med., **1** (2017) 49–54. https://doi.org/10.1016/j.flm.2017.05.002.
44. Koczkur K. M., Mourdikoudis S., Polavarapu L., Skrabalak S. E. – Polyvinylpyrrolidone (PVP) in nanoparticle synthesis. Dalton Trans., **44** (2015) 17883–17905. https://doi.org/10.1039/c5dt02964c.
45. Xu L., Wang Y.-Y., Huang J., Chen C.-Y., Wang Z.-X., Xie H. – Silver nanoparticles: synthesis, medical applications and biosafety. Theranostics, **10** (2020) 8996–9031. https://doi.org/10.7150/thno.45413.
46. Fahad S., Yu H., Wang L., Zain-ul-Abdin, Haroon M., Ullah R. S., Nazir A., Naveed K.-R., Elshaarani T., Khan A. – Recent progress in the synthesis of silver nanowires and their role as conducting materials. J. Mater. Sci., **54** (2019) 997–1035. https://doi.org/10.1007/s10853-018-2994-9.
47. Stec J., Kosikowska U., Mendrycka M., Stępień-Pyśniak D., Niedźwiedzka-Rystwej P., Bębnowska D., Hrynkiewicz R., Ziętara-Wysocka J., Grywalska E. – Opportunistic pathogens of recreational waters with emphasis on antimicrobial resistance—a possible subject of human health concern. Int. J. Environ. Res. Public Health, **19** (2022) 7308. https://doi.org/10.3390/ijerph19127308.
48. Zahedi A., Monis P., Deere D., Ryan U. – Wastewater-based epidemiology-surveillance and early detection of waterborne pathogens with a focus on SARS-CoV-2, *Cryptosporidium* and *Giardia*. Parasitol. Res., **120** (2021) 4167–4188. https://doi.org/10.1007/s00436-020-07023-5.
49. Ramírez-Castillo F., Loera-Muro A., Jacques M., Garneau P., Avelar-González F., Harel J., Guerrero-Barrera A. – Waterborne pathogens: detection methods and challenges. Pathogens, **4** (2015) 307–334. https://doi.org/10.3390/pathogens4020307.